HHS Public Access

Author manuscript

Kidney Int. Author manuscript; available in PMC 2014 December 01.

Published in final edited form as:

Kidney Int. 2014 June ; 85(6): 1382–1394. doi:10.1038/ki.2013.556.

Crk1/2 and CrkL form a hetero-oligomer and functionally complement each other during podocyte morphogenesis

Britta George[#1,2], **Qingfeng Fan**[#1], **Christopher P. Dlugos**[#2], **Abdulsalam A. Soofi**[#3], **Jidong Zhang**[1], **Rakesh Verma**[3], **Tae-Ju Park**[4], **Hetty Wong**[1], **Tom Curran**[4], **Deepak Nihalani**[1], and **Lawrence B. Holzman**[1,5,6]

[1]Renal-Electrolyte and Hypertension Division, University of Pennsylvania, Philadelphia, PA, USA

[2]Medizinische Klinik und Poliklinik D, Universitätsklinikum Münster, Münster, Germany

[3]Division of Nephrology, University of Michigan, Ann Arbor, MI, USA

[4]Department of Pathology and Laboratory Medicine, The Children's Hospital of Philadelphia Research Institute, Philadelphia, PA, USA

[5]Department of Veterans Affair, Philadelphia, PA, USA

[#] These authors contributed equally to this work.

Abstract

Activation of the slit diaphragm protein Nephrin induces actin cytoskeletal remodeling resulting in lamellipodia formation in podocytes *in vitro* in a phosphatidylinositol-3 kinase, focal adhesion kinase, Cas, and Crk1/2-dependent fashion. In mice, podocyte-specific deletion of Crk1/2 prevents or attenuates foot process effacement in two models of podocyte injury. This suggests that cellular mechanisms governing lamellipodial protrusion *in vitro* are similar to those *in vivo* during foot process effacement. Since Crk1/2 null mice develop and aged normally, we tested whether the Crk1/2 paralog, CrkL, functionally complements Crk1/2 in a podocyte-specific context. Podocyte-specific CrkL null mice, like podocyte-specific Crk1/2 null mice, developed and aged normally but were protected from protamine sulfate-induced foot process effacement. Simultaneous podocyte-specific deletion of Crk1/2 and CrkL resulted in albuminuria detected by six weeks post-partum and associated with altered podocyte process architecture. Nephrin-induced lamellipodia formation in podocytes *in vitro* was CrkL-dependent. CrkL formed a heterooligomer with Crk2 and, like Crk2, was recruited to tyrosine phosphorylated Nephrin. Thus, Crk1/2 and CrkL are physically-linked, functionally complement each other during podocyte foot process spreading, and together are required for developing typical foot process architecture.

[6]Corresponding author: Renal-Electrolyte and Hypertension Division 405 Clinical Research Building 415 Curie Boulevard Philadelphia, PA 19104 TEL: 215-573-1831 FAX: 215-898-1830 lholzman@upenn.edu.

Disclosure None

Introduction

Glomerular visceral epithelial cells – also called podocytes – are essential for establishing the permeability characteristics of the kidney filtration barrier. Podocytes surround glomerular capillaries with cellular processes that interdigitate with those of neighboring podocytes. These interdigitating foot processes form a specialized intercellular junction termed the “slit diaphragm”. In most forms of human glomerular disease, podocytes undergo actin cytoskeleton remodeling resulting in foot process spreading and retraction, often described as foot process effacement. Foot process effacement appears to be a common reaction of podocytes to injury or disease stimuli and correlates with the development of albuminuria (1;2).

Several slit diaphragm-associated protein complexes play roles in organizing or remodeling the foot process actin cytoskeleton during normal podocyte development or in response to podocyte injury or disease (3-8). Among these intercellular junction protein complexes is the Nephrin-Neph1 transmembrane receptor complex (9;10). Immunoglobulin superfamily proteins, Nephrin and Neph1 form hetero-oligomeric complexes, associating via *cis*- and *trans*-interactions at the podocyte intercellular junction (9;11). The Nephrin-Neph1 complex cooperate to induce actin filament nucleation and elongation in a tyrosine phosphorylation-dependent fashion at the plasma membrane by recruiting the cytoskeletal adaptor protein Nck1/2 and other proteins of the actin polymerization complex (7;8). Consistent with these observations, mutation of the human gene encoding Nephrin results in Congenital Nephrotic Syndrome of the Finnish-type, a developmental disorder which manifests with heavy proteinuria due to failure of podocyte foot process morphogenesis and their intercellular junctions (12).

In recently published work we provided evidence that Nephrin-induced lamellipodial protrusive activity observed in cell culture employs molecular mechanisms similar to those used in podocyte foot process spreading observed *in vivo*. Nephrin tyrosine phosphorylation was increased with foot process spreading in rodent models of acute podocyte injury and was observed in human glomerular disease. In cell culture, Nephrin tyrosine phosphorylation induced lamellipodial protrusive activity in cultured podocytes in a PI-3 kinase-focal adhesion kinase-p130Cas-Crk1/2-dependent fashion (13). Consent with the hypothesis that this pathway is used *in vivo*, podocyte-specific deletion of Crk1/2 prevented podocyte foot process spreading and proteinuria in two acute podocyte injury models (13). While FAK and p130Cas tyrosine phosphorylation was not observed in podocytes within normal adult human kidney, these proteins were tyrosine phosphorylated in subsets of human glomerular disease. These observations suggest that the FAK-Cas-Crk complex might participate in mediating foot process spreading in some forms of human glomerular disease.

Crk family proteins are ubiquitously expressed SH2 and SH3-domain containing adapter proteins that appear to function in a variety of biological processes including regulation of cell morphology, cell migration, proliferation, and differentiation and may participate simultaneously in a variety of distinct signaling pathways (14). It has been suggested that the functional specificity of the widely deployed Crk proteins is determined primarily by

association with unique upstream receptors and associated protein complexes that are more functionally, temporarily, and anatomically restricted within tissues and within cells (14). Therefore, examining the role of Crk family members within specific cell types should be useful in dissecting functional specificity of Crk-dependent signaling. The Crk family consists of Crk2, its splice isoform Crk1, and its paralog CrkL. Crk1/2 null mouse embryos show defective cardiovascular and craniofacial development while CrkL null mouse embryos exhibit defects in cardiac and neural crest development (15;16). Although the pattern of these defects argues for distinct functional roles of Crk1/2 and CrkL during embryogenesis, several reports suggest that Crk1/2 and CrkL can also execute overlapping functions in a specific cell biological context (17;18). For example, Crk1/2 and CrkL both control neuronal positioning in the developing brain (18).

We reported previously that Crk1/2 is required to transduce a Nephrin activation-dependent signal that results in lamellipodia formation in cultured podocytes (13). Mice with podocyte-specific deletion of Crk1/2 were protected from foot process spreading following acute injury by perfusion with protamine sulfate and in the nephrotoxic serum model of glomerular injury (13). Given the important function of Crk1/2 in cytoskeletal remodeling in other model systems it was surprising that mice with podocyte-specific deletion of Crk1/2 did not show a developmental phenotype or develop a phenotype when aged up to 12 months (19;20). For this reason, we hypothesized that CrkL functionally complements the loss of Crk1/2 in podocytes *in vivo*. The results presented herein support this hypothesis and emphasize the necessity of both Crk1/2 and CrkL during podocyte development and during podocyte injury-induced actin cytoskeletal remodeling.

Results

The cellular distribution of CrkL and Crk 1/2 partially overlap

In pursuit of the hypothesis that CrkL can functionally complement the loss of Crk1/2 in podocytes, we initially investigated whether the two proteins overlap in space. Previously, we showed by indirect immunofluorescence microscopy that Crk1/2 is located diffusely in podocyte cytoplasm *in vivo* and overlaps with Nephrin (Figure 1A and *(13)*). While CrkL is located predominantly in podocyte cell bodies and primary processes, it was also identified in a distribution typical of foot processes (Fig. 1A). Using the same approach we found that the distribution of Crk1/2, CrkL and Nephrin partially overlaps in mouse podocytes (Figure 1A). The cellular distribution pattern of Crk1/2 was unchanged in podocytes that lack CrkL and the cellular distribution pattern of CrkL was unchanged in podocytes that lack Crk1/2 (Fig. 1B and 1C).

Podocyte specific $CrkL^{f/f}$;Podocin-$Cre^{Tg/+}$ mice develop and age normally

CrkL was selectively deleted from mouse podocytes by Cre recombinase-mediated homologous recombination (18;21;22). Podocyte-specific deletion of CrkL was confirmed by indirect immunofluorescence (Fig. 1C). Mice were obtained at the expected Mendelian ratio at birth, developed normally, and exhibited no excessive proteinuria, increased serum creatinine or blood urea nitrogen (BUN) even when aged to 7 months (Fig. 1D).

Podocyte specific CrkL$^{f/f}$;Podocin-Cre$^{Tg/+}$ mice are protected from protamine sulfate-induced podocyte injury

Because CrkL was shown to be involved in mechanisms that determine cytoskeletal dynamics in other model systems, we hypothesized that mice with podocyte-specific deletion of CrkL would show abnormal actin dynamics following injury (19;20). To test this hypothesis, we employed the protamine-sulfate model of podocyte injury since this model induces a signal that results in rapid Crk1/2-dependent cytoskeletal remodeling in podocyte tertiary processes (13;23). Two to three months old podocyte-specific CrkL$^{f/f}$;Podocin-Cre$^{Tg/+}$ mice and control littermates (CrkL$^{f/f}$) were perfused with protamine sulfate or control buffer via their renal arteries, were perfusion fixed and were analyzed by scanning and transmission electron microscopy (Fig. 2A and B). While perfusion of control littermate kidneys with protamine sulfate led to typical foot process spreading, podocytes of podocyte-specific CrkL$^{f/f}$;Podocin-Cre$^{Tg/+}$ mice were protected from protamine sulfate-induced foot process spreading and retraction (Fig. 2A and B). This was confirmed by quantifying podocyte intercellular junction frequency by transmission electron microscopy (Fig. 2B). By this analysis, podocytes of control mice perfused with protamine sulfate had significantly reduced junction frequency while podocyte-specific CrkL null mice perfused with protamine sulfate exhibited normal podocyte intercellular junction frequency similar to control buffer perfused mice. These observations were remarkably similar to results obtained from podocyte-specific Crk1/2 null mice, which were also protected from protamine sulfate-induced podocyte cytoskeletal rearrangement during injury (13). Thus, CrkL like Crk1/2 is necessary for protamine sulfate-induced foot process spreading.

Podocyte-specific Crk1/2 and CrkL double null mice develop abnormally long podocyte foot processes and progressive albuminuria

To examine whether CrkL functionally compensates for the loss of Crk1/2 during podocyte development or maintenance, we generated podocyte-specific double null Crk1/2$^{f/f}$;CrkL$^{f/f}$;Podocin-Cre$^{Tg/+}$ mice by breeding Crk1/2$^{f/f}$ with CrkL$^{f/f}$ mice and crossing the F2 offspring with Podocin-Cre$^{Tg/+}$ mice (16;18;21;22). Mice were obtained at the expected Mendelian ratio at birth. Podocyte-specific deletion of both Crk1/2 and CrkL was confirmed by indirect immunofluorescence (Fig. 3A). Six weeks after birth, podocyte-specific Crk1/2$^{f/f}$;CrkL$^{f/f}$;Podocin-Cre$^{Tg/+}$ mice had significantly higher urine albumin/creatinine ratios than control littermates (Fig. 3B). With aging, the rate of albumin excretion from podocyte-specific Crk1/2;CrkL double null mice increased further while that of control littermates remained unchanged (Fig. 3B). When followed over 7 months, blood urea nitrogen concentration and serum creatinine concentration remained unchanged and were similar to that of control animals despite persistent proteinuria (Fig. 3C). Qualitative analysis of H&E and PAS staining of embedded kidney sections of seven months old podocyte-specific double Crk1/2;CrkL null mice did not show evidence of glomerular hypercellularity or glomerular extracellular matrix accumulation. There were no histological abnormalities observed in the tubular or interstitial compartments (Fig. 4A). Transmission electron microscopy of seven months old podocyte-specific Crk1/2$^{f/f}$;CrkL$^{f/f}$;Podocin-Cre$^{Tg/+}$ mice revealed infrequent patchy alterations consistent with foot process effacement (Fig. 4B). In glomerular areas where no podocyte foot process effacement was observed in podocyte-specific double null mice, podocyte cell process architecture appeared atypical

when examined at 6 weeks and at 7 months post-gestation (Fig. 4C and 4D). Most obvious, podocyte tertiary processes were elongated in double Crk1/2;CrkL null relative to control mice. We devised a method for quantifying tertiary foot process length, which confirmed a statistically significant elongation of tertiary processes in podocyte-specific double null mice compared to controls (Fig. 4E, and see Materials and Methods). We sought to understand why Crk1/2;CrkL null foot processes were elongated by examining glomerular morphology. We considered the possibilities that foot processes were elongated to accommodate potentially dilated glomerular capillaries, a potentially decreased podocyte number per glomerulus and/or a potentially decreased number of major podocyte processes per glomerulus. We measured glomerular capillary widths of control and double Crk null mice using transmission electron micrographs (see Materials and Methods); these glomerular capillary widths did not differ (Fig. 4F). Podocyte number per glomerulus was evaluated using a modified two-thickness method (24). Podocyte-specific $Crk1/2^{f/f}$;$CrkL^{f/f}$;Podocin-$Cre^{Tg/+}$ mice exhibited a small but statistically insignificant decreased number of podocytes per unit glomerulus compared to control mice aged to seven months (Fig. 4G). We then counted the number of secondary podocyte processes per glomerulus using scanning electron micrographs (see Materials and Methods). This showed that podocyte-specific $Crk1/2^{f/f}$;$CrkL^{f/f}$;Podocin-$Cre^{Tg/+}$ mice exhibited approximately half the number of secondary podocyte processes per glomerulus compared to control mice ($Crk1/2^{f/f}$;$CrkL^{f/f}$; Fig. 4H). These surprising observations imply that deletion of both Crk1/2 and CrkL resulted in a defect in podocyte major process branching or a defect in formation of secondary podocyte processes with compensatory elongation of podocyte tertiary processes.

CrkL associates with Nephrin and forms a hetero-oligomer with Crk2

Based on the experiments described above and those previously described by us (13), podocyte-specific deletion of Crk2 or CrkL have indistinguishable phenotypes *in vivo*. Given these observations and cell culture-based evidence that Crk2 is necessary for Nephrin-induced lamellipodia formation, we examined the hypothesis that CrkL-dependent signaling is necessary for Nephrin-induced lamellipodia activity. We used a podocyte cell culture model in which Nephrin tyrosine phosphorylation can be rapidly induced and in which Nephrin tyrosine phosphorylation-mediated signaling events can be readily examined (7;13). A CD16 extracellular domain and a CD7 transmembrane domain were fused with either the Nephrin cytoplasmic domain (NephrinCD) or an HA-tag (negative control) (7;13). CD16/7-NephrinCD or CD16/7-HA was individually co-expressed with CrkL-myc in cultured human podocytes. As described previously, addition of mouse anti-CD16 antibody and a secondary anti-mouse IgG antibody to the media of live cells resulted in tyrosine phosphorylation of CD16/7-NephrinCD within one minute and lamellipodia formation by 30 min (data not shown) (13). When evaluated by confocal microscopy 30 min after addition of the secondary antibody, CrkL-myc was recruited to and co-localized with activated CD16/7-NephrinCD. There was no recruitment of CrkL-myc to CD16/7-HA (Fig. 5A). We expressed CD16NephrinCD and CrkL-his-myc in HEK293 cells. Using Nickel beads, CrkL-his-myc and CD16NephrinCD were pulled down together from HEK293 cell lysate (Fig. 5B). Thus, Nephrin and CrkL, like Nephrin and Crk1/2, occupy the same protein complex.

It was shown previously that CrkL can homo-dimerize via its C-terminal SH3 domain (25). For this reason and because the primary sequences of CrkL and Crk2 are highly conserved, we hypothesized that Crk2 and CrkL might also form a hetero-oligomer via a direct interaction requiring their C-terminal SH3 domains that is required to transduce a signal necessary to induce lamellipodia formation. In initial experiments, CrkL-myc and Crk2-GFP co-expressed in NIH3T3 cells were readily co-immunoprecipitated. In control experiments, CrkL-myc and GFP alone or CrkL-myc and Crk1-GFP (a splice isoform of Crk2, which lacks the C-terminal SH3 domain) did not co-immunoprecipitate (Fig. 5C and 5D). To test whether Crk2 and CrkL interact directly, we expressed and purified recombinant Crk2-His, GST-CrkL or GST from bacteria. In pull down experiments, while GST-CrkL bound to Crk2-His, GST alone did not bind to Crk2-His (Fig. 5E), suggesting that Crk2 and CrkL can bind directly. These results also suggest that Crk2 and CrkL C-terminal SH3 domains play a role in hetero-oligomerization of Crk2 and CrkL.

CrkL and Crk2 are required for Nephrin induced lamellipodia formation

As CrkL is recruited to activated Nephrin and is able to form a hetero-oligomer with Crk2, we examined whether CrkL–like Crk2--is required for Nephrin-induced lamellipodia formation in our CD16/7-NephrinCD model. In addition to a previously described Crk2 deficient podocyte cell line obtained by stable knockdown (KD) of Crk2 (13), a human podocyte cell line with stable knockdown of CrkL was selected after lentiviral infection with an shRNA template (Fig. 6A). Double KD of Crk1/2 and CrkL was established by infecting the stable Crk1/2 KD cell line with CrkL shRNA or by infecting the stable CrkL KD cell line with Crk1/2 shRNA (Fig. 6A). Mock shRNA was used as a control (Fig. 6A). The specificity of the respective Crk1/2 and CrkL antibody was tested in detail (Supp. Figure 1). Upon transient CD16/7-NephrinCD expression and engagement, CrkL-deficient podocytes, like Crk2-deficient podocytes, exhibited attenuated induction of lamellipodial activity relative to controls (Fig. 6B). This CrkL knockdown phenotype was rescued by expressing mouse CrkL in CrkL-knockdown human podocytes (Fig. 6B). Because CrkL and Crk2 were able to compensate the loss of the other protein in podocytes *in vivo* during podocyte maintenance but not during podocyte injury, we analyzed whether CrkL could rescue the Crk2 knockdown phenotype in cultured podocytes and vice versa. Indeed, expression of mouse CrkL in Crk2 KD human podocytes expressing activated CD16/7-NephrinCD rescued Nephrin-induced lamellipodia formation (Fig. 6B). Reciprocally, expression of mouse Crk2 in CrkL knockdown human podocytes rescued Nephrin-induced lamellipodia formation (Fig. 6B). Furthermore, we found that Crk1/2 and CrkL double knockdown human podocytes also did not form lamellipodia following Nephrin activation (Figure 6B). On this double KD background, mouse Crk2 or CrkL—expressed singly—rescued Nephrin-induced lamellipodia formation. Combined expression of both Crk2 and CrkL appeared to rescue Nephrin-induced lamellipodia formation to a greater extent than expression of Crk2 or CrkL alone in double KD cells (Figure 6B). We explored this observation in more detail to test the hypothesis that Crk2 and CrkL behave in synergy in a signaling complex necessary for nephrin activation-induced lamellipodial activity. Expression of increasing quantities of mouse Crk2 and/or CrkL in nephrin-activated double KD human podocytes demonstrated a dose-dependent relationship between Crk plasmid transfected and lamellipodial activity. Importantly, a synergistic relationship between Crk2 and CrkL was

also observed in this model system (Figure 6C and best displayed in Figure 6D). These results imply that Crk1/2 and CrkL are necessary to completely rescue Nephrin-induced lamellipodia formation in Crk1/2 and CrkL double KD podocytes and can partly complement each other functionally. Our results obtained *in vivo* strengthen this conclusion.

Discussion

The podocyte intercellular junction transmembrane protein Nephrin plays a key role integrating podocyte intercellular junction dynamics with podocyte actin cytoskeletal dynamics. Our recently published work suggested that the molecular mechanisms that govern lamellipodial dynamics in cultured podocytes are similar to mechanisms that regulate foot process spreading *in vivo* following injury (13). In both settings, these mechanisms require signaling via a protein complex consisting of Nephrin-FAK-Cas-Crk1/2 (13). The present studies extend our understanding of these mechanisms by demonstrating that CrkL functions in combination with its paralog Crk2 to affect foot process spreading. Evidence derived by biochemical, cellular, and genetic manipulation are consistent, strengthening this conclusion. It is remarkable that podocyte-specific deletion of CrkL results in a complex podocyte phenotype that is indistinguishable from that obtained following podocyte-specific deletion of Crk1/2. Like Crk2, CrkL is recruited to tyrosine phosphorylated Nephrin and is necessary for Nephrin activation-induced lamellipodial activity in cell culture. The additional observation that Crk2 and CrkL physically interact emphasizes the functional interdependence of these adapter proteins in podocyte injury-induced foot process spreading and likely explains the indistinguishable mouse phenotypes obtained when Crk2 or CrkL are knocked out. As Crk1/2 and CrkL are instrumental in fashioning major podocyte processes, it is likely that Crk1/2 and CrkL also fulfill Nephrin-independent functions in the podocyte.

The conclusion that CrkL and Crk2 have overlapping functional roles is consistent with recent observations in other cell systems that suggest that CrkL and Crk1/2 can exhibit context-specific overlapping functional roles (17;18). In the Reelin pathway for example, Crk1/2 and CrkL fulfill essential overlapping functions to control neuronal positioning in the developing brain as mutation of either gene by itself in mice did not compromise Reelin signaling (18). In the podocyte, CrkL and Crk1/2 appear to mediate both context-specific distinct functions and overlapping functions. Despite the observation that both CrkL and Crk1/2 are required for cytoskeletal remodeling following acute podocyte injury, neither CrkL- nor Crk1/2-deficient podocytes *in vivo* showed a discernible morphological phenotype during glomerular development or aging (13). Nevertheless, podocyte-specific deletion of both CrkL and Crk2 resulted in a clearly discernible developmental phenotype. These observations imply that mechanisms driving actin cytoskeletal rearrangement following podocyte injury that lead to foot process spreading are distinct from mechanisms that promote podocyte tertiary process morphogenesis or that regulate actin cytoskeletal dynamics necessary for maintaining podocyte foot process structure in health. These observations are also consistent with the conclusion that podocyte morphogenesis occurs by overlapping function of CrkL and Crk1/2, functions that are subject to functional genetic complementation of one Crk paralog by the other. Understanding the functional role of CrkL and Crk1/2 during podocyte process morphogenesis will be the content of future investigation. During injury-induced podocyte foot process remodeling Crk1/2 and CrkL do

not complement the function of the other since loss of each protein independently results in the same phenotype. Taken in the context of our additional observations that Crk2 and CrkL form directly interacting hetero-dimers and behave in a synergistic fashion in cell culture experiments, we conclude that both proteins act in the same pathway during injury-induced foot process spreading but fulfill distinct roles that are not subject to complementation.

Remarkable similarity exists between the cytoskeletal structure of differentiated neuronal cell processes and podocyte processes (26). Podocyte primary and secondary processes are fashioned by microtubules and intermediate filaments while the structure of tertiary processes is determined by its actin cytoskeleton (27;28). Similarly, the architecture of major neuronal processes is determined by a microtubular meshwork while that of dendritic spines is organized by their actin cytoskeletons (26). As Crk family proteins are required for developing regular major podocyte process architecture as well as for remodeling of podocyte foot processes during injury, this argues that Crk family proteins are instrumental in microtubule- as well as actin-driven podocyte process formation and remodeling. In neurons, Crk and CrkL are necessary for reelin-induced and actin-dependent neurotrophin-induced dendritogenesis (29;30). Furthermore, neurite formation induced by the Cas family member HEF1 requires an intact microtubular system (31). It is intriguing that in neurons as well as in podocytes, Crk or Crk-associated proteins appear to play roles in microtubular- as well as actin-dependent cell process formation/remodeling. Future studies are necessary to dissect the role of Crk family proteins in fashioning major podocyte processes.

Methods

Antibodies and plasmids

Rabbit polyclonal antibody against Nephrin was described previously (7). Rabbit polyclonal antibodies against CrkL (Sigma), c-myc (Sigma), guinea pig polyclonal antibody against Nephrin (Progen Biotechnik) and monoclonal antibodies against CD16 clone 3G8 (BD Pharmingen), Crk (BD Transduction), beta-actin (Sigma), and His (Santa Cruz) were obtained commercially. Plasmids encoding mouse CD16/CD7-NephrinCD, CD16/CD7-HA and actin-GFP were described previously (13). CrkL and Crk2 DNA was amplified from a mouse brain library and cloned into pcDNA3.1MycHis using BamHI and EcoRV restriction sites. The plasmid encoding Crk2-GFP was a gift from Dr. K. Vuori (Sanford-Burnham Medical Research Institute, La Jolla), plasmids encoding Crk2-His and GST-CrkL were gifts form Dr. N. Heisterkamp (Children's Hospital of Los Angeles).

Cell culture and generation of Crk1/2, CrkL, and Crk1/2 and CrkL knockdown cell lines

Conditionally immortalized human podocytes were a gift from Moin Saleem (University of Bristol, UK). Cells were cultured at 33° C as described previously (32). Transient transfections were performed using Lipofectamine 2000 (Invitrogen) according to the manufacturer's instructions. Stable knockdown of CrkL, Crk1/2 or CrkL and Crk1/2 in human podocytes was generated by using the following prepackaged lentivirus-based shRNA oligonucleotides (Mission shRNA Lentiviral Transduction Particles, Sigma): CrkL shRNA
CCGGGACCTGTCTTTGCGAAAGCAACTCGAGTTGCTTTCGCAAAGACAGGTCTT

TTTG; Crk1/2 shRNA CCGGGCTTTACTGGAATTCTACAAACTCGAGTTTGTAGAATTCCAGTAAAGCTTTTT. Puromycin was added to the target cells 24 hours after transduction at a concentration of 2.5 μg/mL.

CD16 chimera, lamellipodia assay, immunoblotting, immunoprecipitation and pull down experiments

Human podocytes were transiently transfected with pEBBCD16/CD7-NephrinCD or pEBBCD16/CD7-HA and pcDNA3.1CrkL-myc-his using Lipofectamine 2000 and following the manufacturer's guidelines. Podocytes were serum-starved in serum-free media for six hours prior to performing the activation assay. Serum-free media containing primary anti-CD16 antibody was added to the podocytes and the cells were incubated on ice for 30 minutes. Cells were then washed with chilled PBS and pre-warmed serum-free media containing Texas Red-labeled secondary goat-anti-mouse IgG was added to the podocytes. Podocytes were then incubated at 37° C for 30 minutes, washed and fixed in 4% PFA solution. Expressed CrkL-myc-his was visualized by indirect immunofluorescence employing rabbit anti-myc-antibody in 2% BSA in PBS-0.1% TX-100 and goat anti-rabbit Alexa488-labeled secondary antibody. Samples were analyzed with a confocal Leica SP5 system with 63× oil immersion objective lens and LAS AF software (Leica) at the Penn Veterinary Medicine Imaging Facility, University of Pennsylvania. Human podocytes positive for lamellipodia were counted employing a previously described protocol (13). For pull down experiments HEK293 cells were transiently transfected with CD16/7-NephrinCD and/or CrkL-his-myc and cell lysates were incubated with Nickel beads. Protocols used for immunoblotting and immunoprecipitation experiments were described previously (7;13).

Indirect immunofluorescence of tissue

Adult mouse kidneys were perfusion-fixed in 4% paraformaldehyde, paraffin embedded and sectioned at a thickness of 4 μm. Indirect immunofluorescence was performed as previously detailed (13). Antigen retrieval was achieved by heating sections to 95° C for 30 minutes in Tris-EDTA buffer (pH 9.0).

CrkL flox mice and Crk1/2;CrkL flox mice

Individual CrkL and Crk1/2 flox mice were previously described (16;18). CrkL flox mice were bred with Cre mice where Cre recombinase is driven by the podocyte-specific podocin promoter (NPSH2) (21;22). To generate mice with floxed genes for CrkL and Crk1/2, CrkL flox mice and Crk1/2 flox mice were crossed. F2 offspring showing the desired genotype of $CrkL^{f/f}$; $Crk1/2^{f/f}$ was then bred with Podocin-Cre mice. For experiments, mice homozygous for the floxed allele CrkL or the alleles CrkL-Crk1/2 ($CrkL^{f/f}$ or $CrkL^{f/f}$;$Crk1/2^{f/f}$) were used as controls while experimental mice in addition to carrying the floxed allele/alleles of CrkL and/or Crk1/2 were heterozygous for Podocin-Cre ($CrkL^{f/f}$;Podocin-$Cre^{Tg/+}$ or $CrkL^{f/f}$;$Crk1/2^{f/f}$;Podocin-$Cre^{Tg/+}$). All animal studies were approved by the University Committee on the Use and Care of Animals Institutional Review Board at the University of Michigan Medical School and the Institutional Animal Care and Use Committee at the University of Pennsylvania. Urine albumin/creatinine ratios were measured using a mouse Albuwell and creatinine kit (Exocell), and an enzyme-linked immunosorbent assay plate

reader (Beckman-Coulter DTX 880 reader). For measuring blood creatinine and BUN, mice were anesthetized, blood was collected in Microtainer serum separator tubes (BD), and was analyzed by the clinical Veterinary School Pathology Laboratory of the University of Pennsylvania.

Protamine sulfate model, electron microscopy and slit diaphragm frequency analysis

Perfusion of podocyte-specific CrkL$^{f/f}$;Podocin-Cre$^{Tg/+}$ mice and control littermates (CrkL$^{f/f}$) was carried out at an age of 8 weeks as previously described (13;23). Preparation of mouse kidneys for scanning or transmission electron microscopy was performed by standard methods using pieces of diced kidney perfused with 4% paraformaldehyde. For SEM, 10-15 glomeruli were analyzed per sample using a Philips XL20 Scanning Electron Microscope at the Cell and Developmental Biology Core, University of Pennsylvania School of Medicine. For TEM, samples were examined with a JEOL 1010 electron microscope at the Electron Microscopy Research Laboratory, University of Pennsylvania School of Medicine. Five to 10 glomeruli per sample were evaluated and slit diaphragm frequency was assessed quantitatively by counting the number of junctions per micron of basement membrane using Image J software.

Measurement of tertiary foot process length, glomerular capillary width, podocyte number per glomerulus and number of secondary podocyte processes per glomerulus

Tertiary foot process length was analyzed by measuring projected foot process length with Image J using SEM images at a magnification of ×10,000. At least three glomeruli of three mice per group were evaluated. The reported glomerular vessel width was determined using TEM images at a magnification of ×3000. We accepted that the measured mean capillary "width" is not equal to the true mean capillary diameter but is smaller because capillaries are not always fully transected. Nevertheless, when a sufficient number of capillary widths are assessed in each glomerulus, differences due to the plane of sectioning converge on a mean that allows comparison between control and mutant mice. Here, at least three glomeruli and multiple capillary loops per glomerulus were evaluated for three mice per group. Podocyte cell number per glomerulus was analyzed employing a modified two thickness method (24). In short, the number of WT-1 positive podocytes and the glomerular area were measured for 30 glomeruli per Crk1/2$^{f/f}$;CrkL$^{f/f}$;Podocin-Cre$^{Tg/+}$ or control mouse using Image J software. The podocyte number was then normalized to the average glomerular volume that was calculated using the Weibel formula. Furthermore, we counted the number of secondary podocyte processes per glomerulus using SEM images at a magnification of ×3000. Secondary processes were identified as the processes that gave rise to foot processes. Glomeruli of three mice per group were evaluated.

Statistics

All data were described as mean ± SEM, and analyzed by using GraphPad Prism 4.03. Statistical analysis was performed by using One-way ANOVA followed by Bonferroni's or Tukey's Multiple Comparison Test. A $p\ value \leq 0.05$ was considered as statistically significant.

Supplementary Material

Refer to Web version on PubMed Central for supplementary material.

Acknowledgements

This work was supported by grants to L.B. Holzman from the NIDDK (DK080751) and the Department of Veterans Affairs, and to B. George from the Deutsche Forschungsgemeinschaft (GE 2158/1-1, GE 2158/3-1). This work was also supported by a Pennsylvania Department of Health Cure Formulary grant to T. Curran (SAP#4100047628).

Reference List

1. Faul C, Asanuma K, Yanagida-Asanuma E, et al. Actin up: regulation of podocyte structure and function by components of the actin cytoskeleton. Trends Cell Biol. 2007; 17:428–437. [PubMed: 17804239]
2. Johnstone DB, Holzman LB. Clinical impact of research on the podocyte slit diaphragm. Nat Clin Pract Nephrol. 2006; 2:271–282. [PubMed: 16932440]
3. George B, Holzman LB. Signaling from the podocyte intercellular junction to the actin cytoskeleton. Semin Nephrol. 2012; 32:307–318. [PubMed: 22958485]
4. Asanuma K, Kim K, Oh J, et al. Synaptopodin regulates the actin-bundling activity of alpha-actinin in an isoform-specific manner. J Clin Invest. 2005; 115:1188–1198. [PubMed: 15841212]
5. Moeller MJ, Soofi A, Braun GS, et al. Protocadherin FAT1 binds Ena/VASP proteins and is necessary for actin dynamics and cell polarization. EMBO J. 2004; 23:3769–3779. [PubMed: 15343270]
6. Reiser J, Polu KR, Moller CC, et al. TRPC6 is a glomerular slit diaphragm-associated channel required for normal renal function. Nat Genet. 2005; 37:739–744. [PubMed: 15924139]
7. Verma R, Kovari I, Soofi A, et al. Nephrin ectodomain engagement results in Src kinase activation, nephrin phosphorylation, Nck recruitment, and actin polymerization. J Clin Invest. 2006; 116:1346–1359. [PubMed: 16543952]
8. Jones N, Blasutig IM, Eremina V, et al. Nck adaptor proteins link nephrin to the actin cytoskeleton of kidney podocytes. Nature. 2006; 440:818–823. [PubMed: 16525419]
9. Barletta GM, Kovari IA, Verma RK, et al. Nephrin and Neph1 co-localize at the podocyte foot process intercellular junction and form cis hetero-oligomers. J Biol Chem. 2003; 278:19266–19271. [PubMed: 12646566]
10. Ruotsalainen V, Ljungberg P, Wartiovaara J, et al. Nephrin is specifically located at the slit diaphragm of glomerular podocytes. Proc Natl Acad Sci U S A. 1999; 96:7962–7967. [PubMed: 10393930]
11. Gerke P, Huber TB, Sellin L, et al. Homodimerization and heterodimerization of the glomerular podocyte proteins nephrin and NEPH1. J Am Soc Nephrol. 2003; 14:918–926. [PubMed: 12660326]
12. Kestila M, Lenkkeri U, Mannikko M, et al. Positionally cloned gene for a novel glomerular protein--nephrin--is mutated in congenital nephrotic syndrome. Mol Cell. 1998; 1:575–582. [PubMed: 9660941]
13. George B, Verma R, Soofi AA, et al. Crk1/2-dependent signaling is necessary for podocyte foot process spreading in mouse models of glomerular disease. J Clin Invest. 2012; 122:674–692. [PubMed: 22251701]
14. Birge RB, Kalodimos C, Inagaki F, et al. Crk and CrkL adaptor proteins: networks for physiological and pathological signaling. Cell Commun Signal. 2009; 7:13. [PubMed: 19426560]
15. Guris DL, Fantes J, Tara D, et al. Mice lacking the homologue of the human 22q11.2 gene CRKL phenocopy neurocristopathies of DiGeorge syndrome. Nat Genet. 2001; 27:293–298. [PubMed: 11242111]
16. Park TJ, Boyd K, Curran T. Cardiovascular and craniofacial defects in Crk-null mice. Mol Cell Biol. 2006; 26:6272–6282. [PubMed: 16880535]

17. Hallock PT, Xu CF, Park TJ, et al. Dok-7 regulates neuromuscular synapse formation by recruiting Crk and Crk-L. Genes Dev. 2010; 24:2451–2461. [PubMed: 21041412]
18. Park TJ, Curran T. Crk and Crk-like play essential overlapping roles downstream of disabled-1 in the Reelin pathway. J Neurosci. 2008; 28:13551–13562. [PubMed: 19074029]
19. Antoku S, Saksela K, Rivera GM, et al. A crucial role in cell spreading for the interaction of Abl PxxP motifs with Crk and Nck adaptors. J Cell Sci. 2008; 121:3071–3082. [PubMed: 18768933]
20. Lamorte L, Rodrigues S, Sangwan V, et al. Crk associates with a multimolecular Paxillin/GIT2/beta-PIX complex and promotes Rac-dependent relocalization of Paxillin to focal contacts. Mol Biol Cell. 2003; 14:2818–2831. [PubMed: 12857867]
21. Moeller MJ, Sanden SK, Soofi A, et al. Two gene fragments that direct podocyte-specific expression in transgenic mice. J Am Soc Nephrol. 2002; 13:1561–1567. [PubMed: 12039985]
22. Moeller MJ, Sanden SK, Soofi A, et al. Podocyte-specific expression of cre recombinase in transgenic mice. Genesis. 2003; 35:39–42. [PubMed: 12481297]
23. Garg P, Verma R, Cook L, et al. Actin-depolymerizing factor cofilin-1 is necessary in maintaining mature podocyte architecture. J Biol Chem. 2010; 285:22676–22688. [PubMed: 20472933]
24. Sanden SK, Wiggins JE, Goyal M, et al. Evaluation of a thick and thin section method for estimation of podocyte number, glomerular volume, and glomerular volume per podocyte in rat kidney with Wilms' tumor-1 protein used as a podocyte nuclear marker. J Am Soc Nephrol. 2003; 14:2484–2493. [PubMed: 14514726]
25. Harkiolaki M, Gilbert RJ, Jones EY, et al. The C-terminal SH3 domain of CRKL as a dynamic dimerization module transiently exposing a nuclear export signal. Structure. 2006; 14:1741–1753. [PubMed: 17161365]
26. Stiess M, Bradke F. Neuronal polarization: the cytoskeleton leads the way. Dev Neurobiol. 2011; 71:430–444. [PubMed: 21557499]
27. Cortes P, Mendez M, Riser BL, et al. F-actin fiber distribution in glomerular cells: structural and functional implications. Kidney Int. 2000; 58:2452–2461. [PubMed: 11115078]
28. Kobayashi N, Mundel P. A role of microtubules during the formation of cell processes in neuronal and non-neuronal cells. Cell Tissue Res. 1998; 291:163–174. [PubMed: 9426305]
29. Matsuki T, Pramatarova A, Howell BW. Reduction of Crk and CrkL expression blocks reelin-induced dendritogenesis. J Cell Sci. 2008; 121:1869–1875. [PubMed: 18477607]
30. Nakamura T, Komiya M, Sone K, et al. Grit, a GTPase-activating protein for the Rho family, regulates neurite extension through association with the TrkA receptor and N-Shc and CrkL/Crk adapter molecules. Mol Cell Biol. 2002; 22:8721–8734. [PubMed: 12446789]
31. Bargon SD, Gunning PW, O'Neill GM. The Cas family docking protein, HEF1, promotes the formation of neurite-like membrane extensions. Biochim Biophys Acta. 2005; 1746:143–154. [PubMed: 16344118]
32. Saleem MA, O'Hare MJ, Reiser J, et al. A conditionally immortalized human podocyte cell line demonstrating nephrin and podocin expression. J Am Soc Nephrol. 2002; 13:630–638. [PubMed: 11856766]

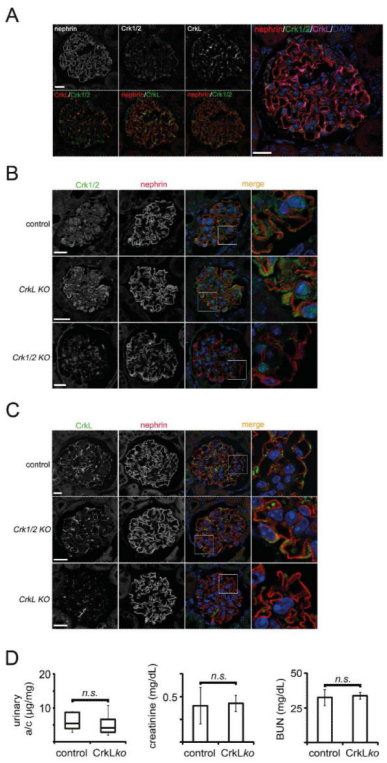

Figure 1.

CrkL and Crk1/2 co-localize with Nephrin at the podocyte slit-diaphragm and podocyte-specific CrkL$^{f/f}$;Podocin-Cre$^{Tg/+}$ mice develop and age normally. (A) Paraffin-embedded wild-type kidney sections were stained for Nephrin, Crk1/2 and CrkL (upper panel). Merged images of either CrkL (red) and Crk1/2 (green), Nephrin (red) and CrkL (green) or Nephrin (red) and Crk1/2 (green) are shown in the lower panel. A merged image of Nephrin (red), Crk1/2 (green), CrkL (purple), and DAPI (blue) staining is presented in the far right panel. Scale bars: 20 µm. (B and C) Control, podocyte-specific Crk1/2$^{f/f}$;Podocin-Cre$^{Tg/+}$ (Crk1/2 *KO*) or podocyte-specific CrkL$^{f/f}$;Podocin-Cre$^{Tg/+}$ (CrkL *KO*) mice were stained for Crk1/2 (green, B) or CrkL (green, C), Nephrin (red) and DAPI (blue). Higher magnifications of part of a glomerulus are shown in the far right panel. Scale bars: 20 µm. (D) Left: Boxplot showing the median, first and third interquartile ranges as well as the minimum and maximum of urinary albumin/creatinine ratios (a/c) of control (CrkL$^{f/f}$) and podocyte-specific CrkL$^{f/f}$;Podocin-Cre$^{Tg/+}$ mice at the age of 6 months (albumin:creatinine values in µg/mg of 4-5 mice). Middle: Statistical analysis of serum creatinine levels of control and podocyte-specific CrkL$^{f/f}$;Podocin-Cre$^{Tg/+}$ mice at the age of 6 months (means +/− SEM of blood creatinine values in mg/dL of 6-8 mice). Right: Statistical analysis of blood urea nitrogen (BUN) levels of control and podocyte-specific CrkL$^{f/f}$;Podocin-Cre$^{Tg/+}$ mice at the age of 6 months (means +/− SEM of BUN values in mg/dL of 6-8 mice). (n.s.: not significant).

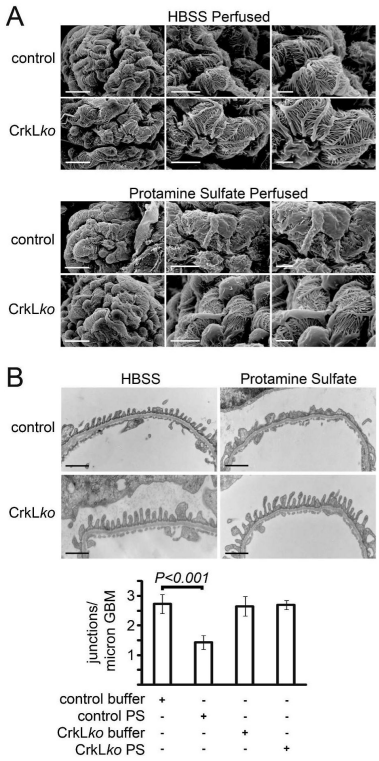

Figure 2.

Podocyte-specific CrkL$^{f/f}$;Podocin-Cre$^{Tg/+}$ mice are protected from protamine sulfate-induced podocyte injury. (A and B) Scanning or transmission electron microscopy (EM) images of podocytes of control (CrkL$^{f/f}$) or podocyte-specific CrkL$^{f/f}$;Podocin-Cre$^{Tg/+}$ (CrkLko) mice perfused with HBSS or protamine sulfate (PS). Results are representative of 3-4 mice per group. At the bottom the number of podocyte intercellular junctions per micron glomerular basement membrane (GBM) as seen by transmission EM is shown (B). Data represent means +/− SEM. Scale bars: 10 μm (left column, A), 5 μm (middle column, A), 2 μm (right column, A); 1 μm (B).

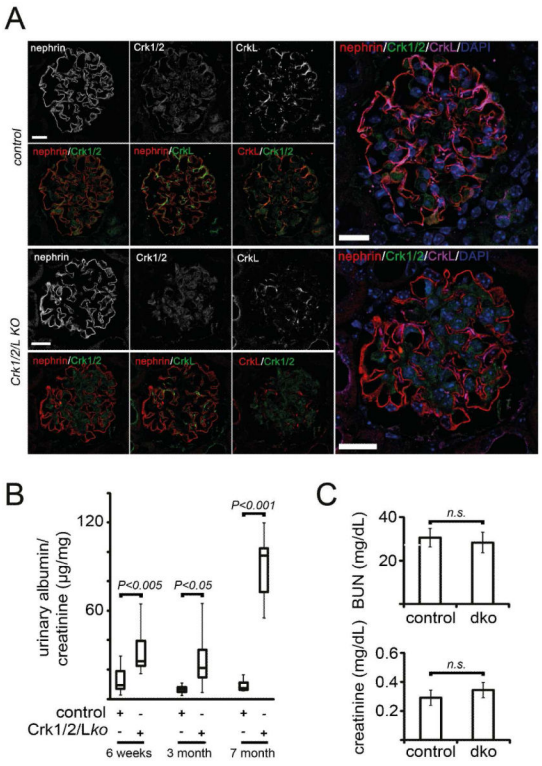

Figure 3.

Podocyte-specific Crk1/2$^{f/f}$;CrkL$^{f/f}$;Podocin-Cre$^{Tg/+}$ mice develop a progressive albuminuria. (A) Paraffin-embedded kidney sections of control (Crk1/2$^{f/f}$;CrkL$^{f/f}$) or podocyte-specific Crk1/2$^{f/f}$;CrkL$^{f/f}$;Podocin-Cre$^{Tg/+}$ (Crk1/2/L *KO*) mice were stained for Nephrin, Crk1/2, CrkL and DAPI. Merged images of Nephrin (red) and Crk1/2 (green), Nephrin (red) and CrkL (green) or CrkL (red) and Crk1/2 (green) are shown in the second and fourth row. Merged images of Nephrin (red), Crk1/2 (green), CrkL (purple) and DAPI (blue) are shown in the far right panel. Scale bars: 20 µm. (B) Boxplot showing the median, first and third interquartile ranges as well as the minimum and maximum of urinary albumin/creatinine ratios of control (Crk1/2$^{f/f}$;CrkL$^{f/f}$) and podocyte-specific Crk1/2$^{f/f}$;CrkL$^{f/f}$;Podocin-Cre$^{Tg/+}$ mice at the age of 6 weeks, 3 months and 7 months in µg/mg (albumin/creatinine values of 6-12 mice per group). (C) Upper graph: Statistical analysis of blood urea nitrogen (BUN) levels of control and podocyte-specific Crk1/2$^{f/f}$;CrkL$^{f/f}$;Podocin-Cre$^{Tg/+}$ mice at the age of 7 months in mg/dL (means +/− SEM of BUN values of 9-11 mice per group). Lower graph: Statistical analysis of serum creatinine levels of control and podocyte-specific Crk1/2$^{f/f}$;CrkL$^{f/f}$;Podocin-Cre$^{Tg/+}$ (dko) mice at the age of 7 months in mg/dL (means +/− SEM of serum creatinine values of 9-11 mice per group). P value as indicated; n.s.: not significant.

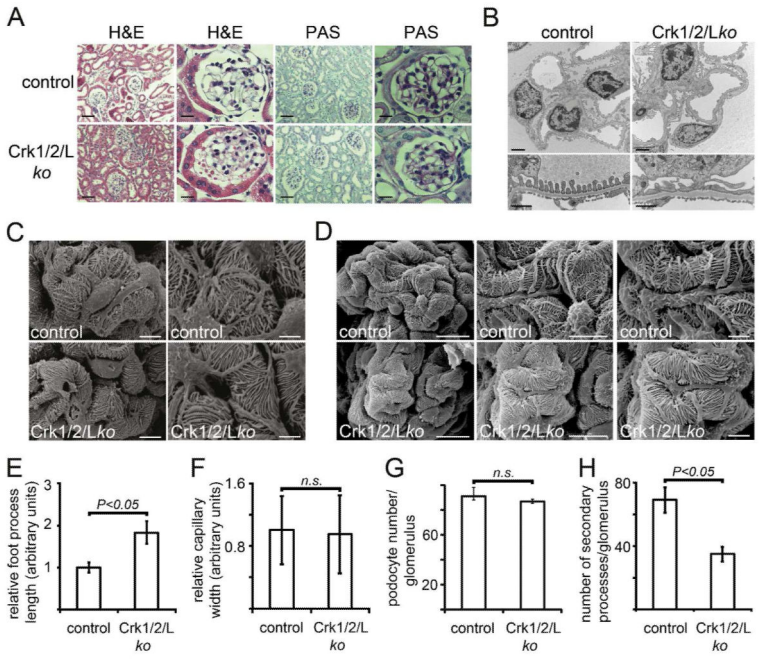

Figure 4.

Podocyte-specific Crk1/2$^{f/f}$;CrkL$^{f/f}$;Podocin-Cre$^{Tg/+}$ mice exhibit abnormally long foot processes and a decreased number of secondary podocyte processes per glomerulus. (A) Paraffin-embedded kidney sections of control (Crk1/2$^{f/f}$;CrkL$^{f/f}$) or podocyte-specific Crk1/2$^{f/f}$;CrkL$^{f/f}$;Podocin-Cre$^{Tg/+}$ (Crk1/2/Lko) mice at the age of 7 months were stained with hematoxilin&eosin (H&E) or Periodic Acid Schiff (PAS). Scale bars: 60 μm (first and third column from left) and 20 μm (second and forth column from left). (B) Transmission electron microscopy (EM) images of control or podocyte-specific Crk1/2$^{f/f}$;CrkL$^{f/f}$;Podocin-Cre$^{Tg/+}$ mouse glomeruli at the age of 7 months. Scale bars: 5 μm (upper panel), 1 μm (lower panel). (C and D) Scanning EM images of control or podocyte-specific Crk1/2$^{f/f}$;CrkL$^{f/f}$;Podocin-Cre$^{Tg/+}$ mouse glomeruli at the age of 6 weeks (C) or 7 months (D). Scale bars: 4 μm (left column, C), 2 μm (right column, C); 10 μm (left column, D), 5 μm (middle column, D), 2 μm (right column, D). (E) Statistical analysis of relative tertiary process length of podocyte-specific Crk1/2$^{f/f}$;CrkL$^{f/f}$;Podocin-Cre$^{Tg/+}$ mouse podocytes normalized to controls as seen by transmission EM. (F) Statistical analysis of relative glomerular capillary widths of podocyte-specific Crk1/2$^{f/f}$;CrkL$^{f/f}$;Podocin-Cre$^{Tg/+}$ mice normalized to controls as seen by transmission EM. (G) Podocyte number per glomerulus of control mice or podocyte-specific Crk1/2$^{f/f}$;CrkL$^{f/f}$; Podocin-Cre$^{Tg/+}$ mice. (F) Statistical analysis of the number of secondary podocyte processes per glomerulus of control or podocyte-specific Crk1/2$^{f/f}$;CrkL$^{f/f}$;Podocin-Cre$^{Tg/+}$ mice as seen by scanning EM. Shown are means +/− SEM (n.s., not significant; P value as indicated). Results are representative of at least 3 mice per group.

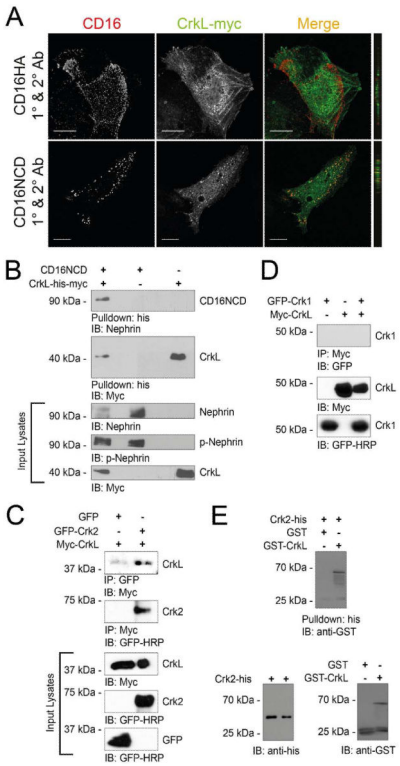

Figure 5.

CrkL associates with Nephrin and forms a hetero-oligomer with Crk2. (A) Cultured human podocytes expressing CD16/7-NephrinCD (CD16NCD) or CD16/7-HA (CD16HA) and CrkL-myc were activated by addition of monoclonal anti-CD16 primary antibody (1°) and goat anti-mouse IgG Texas Red-conjugated secondary antibody (2°) to the media of live cells. CrkL-myc was detected with rabbit polyclonal anti-myc primary antibody and Alexa Fluor 488-labeled secondary antibody. Cells were analyzed by confocal microscopy. Note that CD16/7-NephrinCD (red) and CrkL-myc (green) co-localize. Scale bars: 20 μm. yz plane reconstructions are shown at the far right. (B) Lysates of cultured HEK293 cells expressing CD16/7-NephrinCD and/or CrkL-His-myc were incubated with Nickel beads. (C and D) Co-immunoprecipitation and immunoblots using indicated antibodies demonstrated that Crk2-GFP and Myc-CrkL co-immunoprecipitated (C) while Myc-CrkL and GFP alone (C) or Myc-CrkL and Crk1-GFP (D) did not co-immunoprecipitate. (E) Crk2-His, GST and GST-CrkL were expressed in BL21 E. coli. Purified recombinant Crk2-His was incubated with either GST or GST-CrkL and pulled down using Nickel beads demonstrating that Crk2-His and GST-CrkL interacted directly. Results are representative of at least 3 independent experiments.

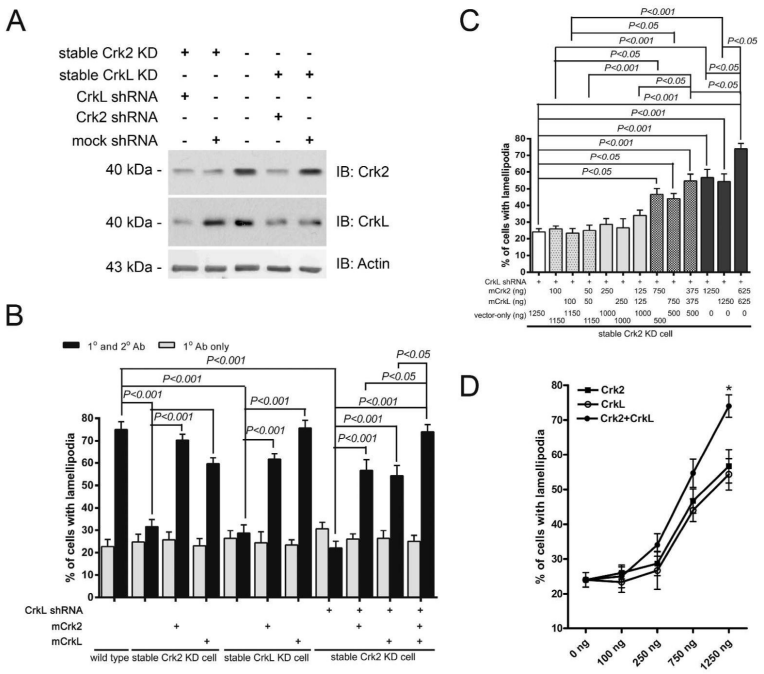

Figure 6.

CrkL like Crk2 is required for Nephrin-induced lamellipodia formation. (A) Immunoblot demonstrating specific attenuation by knockdown of CrkL, Crk2, or CrkL and Crk2 expression in human podocyte cell lines. Scrambled shRNA was used as control. (B) Podocytes expressing plasmid encoding CrkL or Crk2 shRNA or both were transfected with CD16/7-NephrinCD, and mouse Crk2 (mCrk2) or mouse CrkL (mCrkL) or both as indicated and activated by clustering as described in Figure 5. The fraction of cells exhibiting lamellipodial protrusions was evaluated after fixation. (C) Crk2 and CrkL function in a synergistic fashion. The Crk1/2;CrkL double knockdown human podocytes were rescued with different amounts of Crk2, CrkL, or Crk2 + CrkL by transiently transfecting the human podocytes stably expressing Crk2 shRNA (stable Crk2 KD cell) with plasmids encoding CD16/7-NephrinCD, CrkL shRNA and indicated quantities of plasmids (x-axis) encoding mouse Crk2 and/or CrkL. Cells were activated by clustering. The fraction of cells showing lamellipodia protrusions were determined after fixation and are represented as bars. The synergistic enhancement of lamellipodia formation was noted when either 375ng or 625ng of each of Crk2 and CrkL plasmids were used in this assay. The line graph presented in D further confirms the observations from figure C. (D) *P<0.05, Crk2 + CrkL vs. Crk2 or CrkL. (B and C) Note that total quantity of plasmid used for each condition was maintained equal by addition of appropriate amounts of empty expression plasmid. Results are representative of 3 independent experiments and are shown as means +/− SEM. P values as indicated and were significant in each case.